

THEORY, TECHNOLOGY AND ASSEMBLY OF A HIGHLY SYMMETRICAL CAPACITIVE TRIAXIAL ACCELEROMETER

J.C. Lötters, W. Olthuis, P.H. Veltink, P. Bergveld

MESA Research Institute, University of Twente

P.O. Box 217, 7500 AE Enschede, The Netherlands

Phone: +31-53-4892755; Fax: +31-53-4892287; e-mail: j.c.lotters@el.utwente.nl

ABSTRACT

A highly symmetrical cubic easy-to-assemble capacitive triaxial accelerometer for biomedical applications has been designed, realized and tested. The outer dimensions of the sensor are $5 \times 5 \times 5 \text{ mm}^3$ and the device is mounted on a standard IC package. New aspects of the sensor are an easy assembly procedure, the use of the polymers polydimethylsiloxane (PDMS) as spring material between the capacitor plates and the mass and polyimide (PI) as flexible interconnection layer between the capacitor plates, and the highly symmetrical cubic structure. The mathematical model, technology and assembly procedure of the sensor are described. The measurement results show a good linearity in the output voltage for accelerations up to at least 5 g and a bandwidth of DC - >50 Hz. In the x-axis the sensitivity was found to be 175 mV/g which is in good correspondence with the theory. The sensitivity can be increased when the PDMS layer is patterned, which was shown in previous versions of the highly symmetrical triaxial accelerometer.

INTRODUCTION

There is a need for very small triaxial accelerometers in the biomedical field. These sensors can for instance provide kinematic information for the control of mobility in paraplegic patients [1] and enable the ambulant monitoring of movement disorders of patients suffering from Parkinson's disease [2]. The most important specifications for biomedical applications are [3]: amplitude range $\pm 5 \text{ g}$, resolution 1 mg, bandwidth DC-50 Hz, off-axis sensitivity < 5% g/g, dimensions $\sim 2 \times 2 \times 2 \text{ mm}^3$ and power consumption < 1 mW.

Up to now, triaxial accelerometers presented in the literature [4,5] have a lack of symmetry and therefore show a large off-axis sensitivity from 5 % up to 21% [4]. The sensor proposed in this paper has a highly symmetrical configuration, consisting of a central cubic mass surrounded by capacitors, which ideally should not result in any off-axis sensitivity. Furthermore, due to the high degree of symmetry and differential measuring,

common mode interferences as introduced by temperature fluctuations, electric and magnetic fields, humidity and other disturbing effects should be rejected. In this paper the sensor structure, its theoretical model, technology, assembly procedure and some measurement results are described.

THEORY

Sensor Structure

The basic concept of the sensor consists of capacitors surrounding one central cubic tungsten mass (figure 1a), two capacitors per side (figures 1b, 2b). The mass is suspended to the fixed capacitor plates by springs made of polydimethylsiloxane (PDMS). The capacitors which sense the occurring accelerations will be connected to a capacitance to voltage converter (CVC) which needs a high frequency excitation voltage, $V_{in} [\text{V}]$ (figure 4).

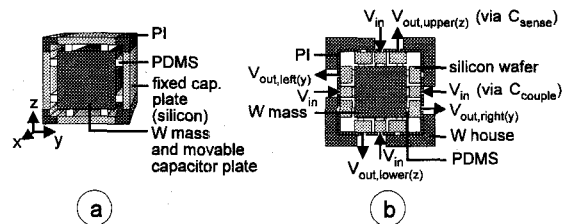


Figure 1. Basic structure of the triaxial accelerometer, cross-sectional (a) 3D view, (b) 2D view

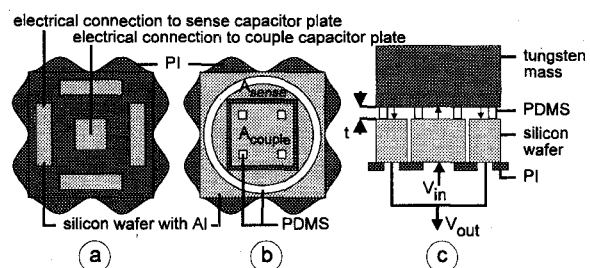


Figure 2. (a) Rear view and (b) front view of one of the six outer capacitor plates; (c) two-dimensional cross-sectional view of a part of the basic structure of the symmetrical cubic triaxial accelerometer

From each side, the inner capacitor is used to capacitively couple the excitation voltage to the seismic mass and the outer capacitor is used to sense the applied accelerations (figure 1b). When an acceleration is applied, the mass moves with respect to the fixed capacitor plates due to the flexibility of the PDMS structures and the values of the capacitance are changed. Neglecting fringing effects, the value of the capacitance of the couple capacitor (figure 2b) when no acceleration is applied $C_{couple,side,0}$ [F] of each side can be equated with

$$C_{couple,side,0} = \frac{\epsilon_0(A_{couple} - A_{PDMS,couple}) + \epsilon_0\epsilon_r A_{PDMS,couple}}{t_{side}} \quad (1)$$

with ϵ_0 [F/m] the dielectric constant of vacuum ($\epsilon_0 = 8.85 * 10^{-12}$ [F/m]), ϵ_r the relative dielectric constant of PDMS, $A_{PDMS,couple}$ [m²] the area of the PDMS on the couple capacitor plate, A_{couple} [m²] the area of the couple capacitor plate and t_{side} [m] the nominal distance between the capacitor plates and the mass.

When the couple capacitor from only one side would be used, the couple capacitance would change and the output voltage of the CVC would vary with this capacitance, which is an undesired effect. Fortunately, due to the symmetry of the design, when all couple capacitances are used in parallel, the total couple capacitance $C_{couple,total}$ [F] will remain constant, independent of the applied acceleration. $C_{couple,total}$ [F] can be equated with $C_{couple,total} = 6C_{couple,side,0}$ under the assumption that the variation in t_{side} is less than 1%.

The six sides of the triaxial accelerometer will be indicated as left(x), right(x), left(y), right(y), upper(z) and lower(z). When the sensor structure is fully symmetrical, the sense capacitances between the capacitor plates and the central cubic mass have an equal nominal capacitance value $C_{sense,side,0}$ [F] of

$$C_{sense,side,0} = \frac{\epsilon_0(A_{sense} - A_{PDMS,sense}) + \epsilon_0\epsilon_r A_{PDMS,sense}}{t_{side}} \quad (2)$$

with $A_{PDMS,sense}$ [m²] the area of the PDMS on the sense capacitor plate and A_{sense} [m²] the area of the sense capacitor plate. The total sense capacitance $C_{sense,total}$ [F] consists of all six sense capacitors in parallel and will remain constant independent of the applied acceleration. $C_{sense,total}$ can be equated with $C_{sense,total} = 6C_{sense,side,0}$, when the variation in t_{side} is less than 1%.

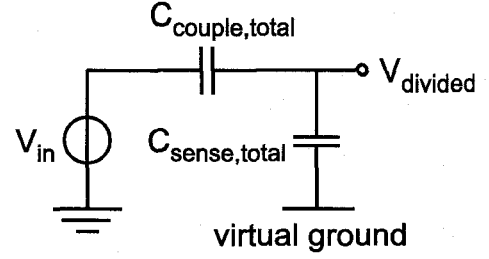


Figure 3. Voltage divider

$C_{sense,total}$ and $C_{couple,total}$ divide the input voltage of the capacitance to voltage converter (CVC) as shown in figure 3. The voltage dividing effect can be overcome by choosing each feedback capacitor C_f [F] of the CVC as shown in figure 4

$$C_f = \frac{C_{couple,total}}{C_{sense,total} + C_{couple,total}} \cdot C_{sense,side,0} \quad (3)$$

The nominal distance t_{side} between the capacitor plates and the central mass is determined by the thickness of the PDMS structure. When an acceleration is applied, the mass moves a distance Δt [m] with respect to the fixed outer capacitor plates, resulting in a corresponding capacitance change ΔC [F]. For instance, when the acceleration is applied in the +z-direction, the distance between the mass and the upper capacitor plate increases to $t_{upper(z)} + \Delta t_z$ and the distance between the mass and the lower capacitor plate decreases to

$t_{lower(z)} - \Delta t_z$. So, the upper capacitance $C_{sense,upper(z)}$ [F] is decreased and the lower capacitance $C_{sense,lower(z)}$ [F] is increased:

$$\begin{aligned} C_{sense,upper(z)} &= \frac{C_{sense,upper(z),0} \cdot t_{upper(z)}}{t_{upper(z)} + \Delta t_z} \\ &= C_{sense,upper(z),0} - \Delta C_{sense,upper(z)} \end{aligned} \quad (4)$$

$$\begin{aligned} C_{sense,lower(z)} &= \frac{C_{sense,lower(z),0} \cdot t_{lower(z)}}{t_{lower(z)} - \Delta t_z} \\ &= C_{sense,lower(z),0} + \Delta C_{sense,lower(z)} \end{aligned} \quad (5)$$

When the sensor is fully symmetrical, $t_{upper(z)} = t_{lower(z)} = t_z$ and thus both the upper and the lower nominal capacitances have an equal nominal value $C_{sense,z,0}$. Furthermore, when $\Delta t_z < 0.01t_z$, both capacitors will be varied with the same $\Delta C_{sense,z} = \Delta C_{sense,upper(z)} = \Delta C_{sense,lower(z)}$. Therefore,

$$\Delta C_{sense,z} = \frac{C_{sense,z,0} \cdot \Delta t_z}{t_z} \Rightarrow \frac{\Delta C_{sense,z}}{C_{sense,z,0}} = \frac{\Delta t_z}{t_z} \quad (6)$$

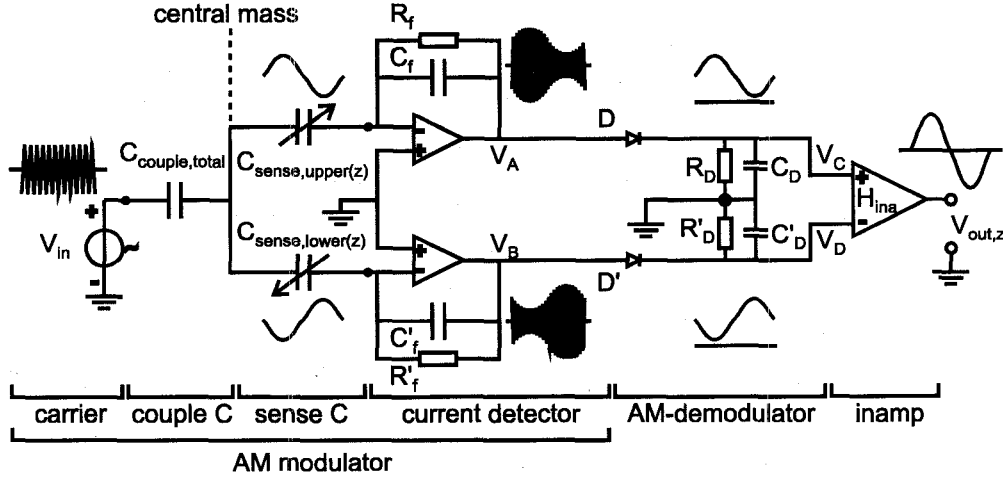


Figure 4. Differential capacitance to voltage converter (CVC); a second and a third identical CVC are connected to the x- and y- axis sense capacitors

When the triaxial accelerometer is connected to the differential CVC of figure 4, the output voltage $V_{out,z}$ [V] due to an applied acceleration a_z [m/s²] in the z-direction is

$$\begin{aligned}
 V_{out,z} &= H_{ina} \hat{V}_{in} \frac{C_{couple,total}}{C_{couple,total} + C_{sense,total}} \frac{2\Delta C_{sense,z}}{C_f} \\
 &= H_{ina} \hat{V}_{in} \frac{C_{couple,total}}{C_{couple,total} + C_{sense,total}} \frac{C_{sense,z,0}}{C_f} \frac{2\Delta t_z}{t_z} \\
 &= H_{ina} \hat{V}_{in} \frac{C_{couple,total}}{C_{couple,total} + C_{sense,total}} \frac{C_{sense,z,0}}{C_f} \frac{2ma_z}{k_{total,z} \cdot t_z}
 \end{aligned} \quad (7)$$

with H_{ina} the gain of the instrumentation amplifier, m [kg] the seismic mass and $k_{total,z}$ [N/m] the spring constant in the z-axis. Corresponding equations can be derived for the output voltage in the y and z-direction.

Spring constant of the triaxial accelerometer

For small simple extension and uniaxial compression ($\Delta t_{CE} / t_{side} < 0.01$), the spring constant k_{CE} [N/m] of a rubberelastic structure as shown in figure 5a can be equated with [7]

$$k_{CE} = F_{CE} / \Delta t_{CE} = 3 A_R G / t_{side} \quad (8)$$

with F_{CE} [N] the applied compressive or extensive force [N], A_R [m²] the area of the rubber on which the force is applied (in the case of PDMS this area is called A_{PDMS} which is equal to $A_{PDMS,sense} + A_{PDMS,couple}$), G [Pa] the shear modulus of the rubber, Δt_{CE} [m] the change in thickness of the rubber due to F_{CE} .

The shear spring constant k_{SH} [N/m] can be equated with (figure 5b) [7]

$$k_{SH} = F_{SH} / \Delta t_{SH} = A_R G / t_{side} \quad (9)$$

with F_{SH} [N] the applied shear force and Δt_{SH} [m] the corresponding change in thickness.

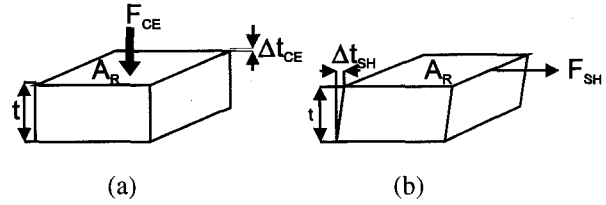


Figure 5. Piece of rubberelastic material on which (a) a compressive or extensive force or (b) a shear force is applied

The total spring constant k_{total} [N/m] in one axis is [7]

$$k_{total} = 2 \cdot k_{CE} + 4 \cdot k_{SH} = 10 \cdot A_{PDMS} G / t_{side} \quad (10)$$

Equation (10) can be used for all axes (x, y and z) of the triaxial accelerometer provided that the sensor is fully symmetrical. Otherwise, the differences in the layer thickness should be taken into account [7].

EXPERIMENTAL

Cleanroom technology

A silicon wafer was oxidized applying wet nitrogen for 5 hours at 1150°C resulting in 1.4 μm SiO₂. The front side of the wafer and the outer ring of the back side were covered with positive photoresist S1818 of Shipley. The silicon oxide was etched from the uncovered part of the back side of the wafer during 25 minutes in 50% buffered HF. The photoresist was removed in fuming

nitric acid. The silicon at the back side was etched during 5 hours in KOH at 76 °C so that a silicon membrane remained of about 100 μm (figure 6a). This was done to decrease the RIE etch time in the last process step and to obtain minimum dimensions. An aluminium layer of 300 nm was deposited on both sides of the wafer by evaporation and was annealed for 30 minutes at 450 °C applying wet nitrogen, to eventually obtain an ohmic contact between gold bond wires and the capacitor plates (figure 6b). A chromium layer of 200 nm was deposited on the back side of the wafer by evaporation to act as an adhesive for the polyimide (figure 6c). At the back of the wafer, polyimide (PI, HTR3-2000 of OCG) was spincoated and patterned to obtain the structure as displayed in figures 2a and 7 with a height of 15 μm. At the front side, PDMS was spincoated. The processing of PDMS PS851 of ABCR and its properties after cross-linking are described in [7] and [8]. Ten percent of TMSM and a half percent of demi-water were solved in xylene and the mixture was heated up to 60°C. The wafers were kept in this mixture for one minute so that methacryl groups were present at the wafer surface, which will attach to the methacryl groups of the PDMS. The wafer was rinsed with demi-water to remove the surplus of TMSM and was spun dry. The PDMS was spun upon the wafer with a spin rate of 3000 rpm during 60 seconds. After the spinning, the PDMS layer was covered with Mylar foil of 23 μm to avoid sticking of the PDMS to the mask and to keep oxygen away from the PDMS (otherwise no cross-linking will take place). Thereafter, the PDMS was exposed to UV light for 40 s via a mask, to obtain the desired structures as displayed in figure 2b (however, in the device described in this paper, the patterning of the PDMS was not performed, because the protective chromium layer could not be successfully deposited so that the patterned PDMS was removed during the RIE etching). Subsequently, the Mylar foil was removed and the PDMS was developed in xylene for 30 s, rinsed with isopropanol and spun dry (figure 6e). The thickness of the PDMS structures was about 12 μm. The front side was covered with a chromium layer of 50 nm in order to protect the PDMS structures against the RIE etching (figure 6f). The aluminium and chromium layers at the front side are covered with positive photoresist where all the capacitor plates should be separated by RIE etching. The uncovered metal parts are etched with aluminium and chromium etchant, respectively. Both the capacitor plates and the crosses were separated by RIE etching, using the black silicon method [9]. It took 1 hour to etch through the wafer (figure 6g). After the RIE etching, all the cross-wise structures were available (figure 7). The protective aluminium and chromium layers were removed with aluminium and chromium etchant, respectively, and the structures were ready to be assembled (figure 6h).

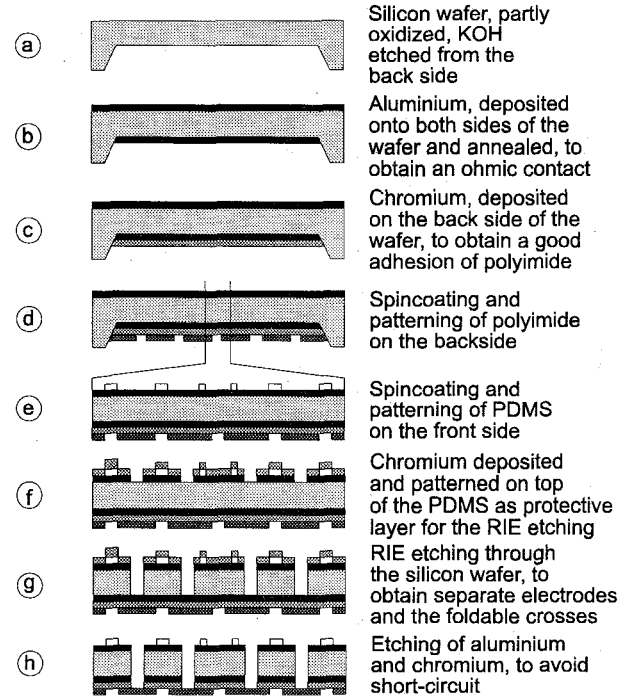


Figure 6. Process steps of the triaxial accelerometer: from silicon wafer to foldable cross structure

All appropriate dimensions, material properties and CVC data are shown in table I.

Table I. Dimensions, material properties and CVC data

seismic mass	$m = 520$ mg (cubic piece of tungsten) edge $e = 3$ mm
PDMS	$A_{PDMS, sense} = 6.75 \cdot 10^{-6}$ m ² $A_{PDMS, couple} = 2.25 \cdot 10^{-6}$ m ² $G = 250$ kPa $\epsilon_r = 2.5$ $t = 12$ μm
capacitor/side	outer length $l = 3$ mm length couple plate $l_{cp} = 1.5$ mm sense area $A_{sense} = 6.75 \cdot 10^{-6}$ m ² couple area $A_{couple} = 2.25 \cdot 10^{-6}$ m ² $C_{sense, side, 0} = 12.5$ pF $C_{couple, side, 0} = 4.2$ pF
CVC	$C_f = 4$ pF $H_{ina} = 50$ $\hat{V}_{in} = 10$ V

Assembly procedure

The cubic tungsten mass was cleaned with ethanol. The cross-wise connected wafer pieces were put on the assembly device and the mass was placed on the central wafer piece, as shown in figure 8. The flexible PI layer (figures 2a and 7) can easily be folded into the desired shape, making the assembly procedure really easy [10].

The four capacitor plates at the sides of the mass were pushed onto the corresponding sides of the mass by bending the PI layer with the push bars. The PDMS will stick to tungsten [8], no glue is necessary. The last capacitor plate was pushed onto the top of the mass and the thus formed cube was put inside a tungsten house which was put upon a standard IC package (figure 9). The tungsten cover was glued upon the tungsten house and gold bond wires were attached from the IC package to the sensor via slits in the tungsten house.

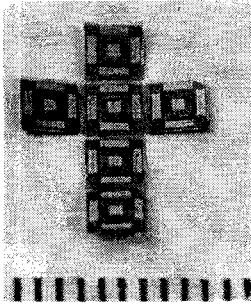


Figure 7. Six sides of the foldable device, each containing two capacitor plates, cross-wise connected by polyimide, on a mm scale (see also figure 2a)

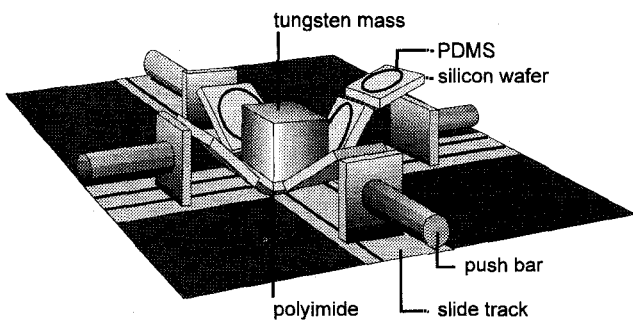


Figure 8. Assemble device for the accelerometer

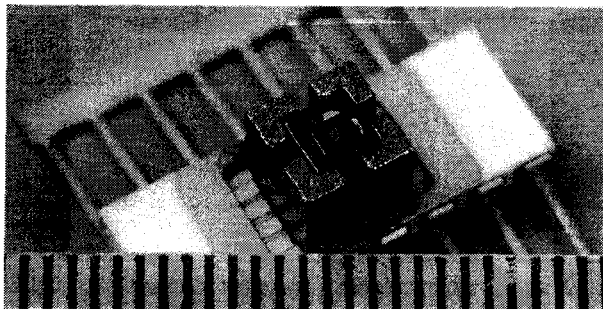


Figure 9. Folded triaxial accelerometer in a tungsten house on a standard IC package. Gold bond wires are attached via the slits in the side walls of the house

Measurement protocol

The devices were statically tested by turning their sensitive axes with respect to gravity and dynamically tested by applying known accelerations (reference accelerometer Piezotronics ICP-301A10) with a shaker unit (Gearing and Watson GWV20).

RESULTS AND DISCUSSION

The device as shown in figure 9 was put upon the shaker unit and its linearity and frequency response were measured. The linearity of the device is shown in figure 10 and the bandwidth was found to be DC - > 50 Hz. When the data of table I are substituted in equation (7), a sensitivity of 175 mV/g is obtained for all axes. As can be seen in figure 10, the measured sensitivity of the x-axis shows a good correspondence with the theoretical sensitivity. Furthermore, the output voltage of all axes increases linearly with the applied acceleration, as was expected.

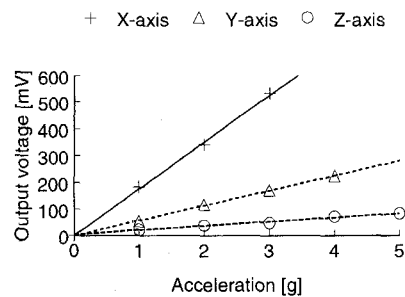


Figure 10. Calculated (solid line) and measured (markers) output voltage of the triaxial accelerometer per axis versus the applied acceleration

However, the sensitivity in the y- and z-axis, 55 mV/g and 17 mV/g, respectively, is less than predicted by the theory. The lower sensitivity in the y-axis is probably caused by a larger distance between the mass and the capacitor plates and the lower sensitivity in the z-axis is probably caused by a high pressure of the tungsten cover on the PDMS which senses in the z-direction.

In this sensor, the PDMS layer was not patterned, so both the couple and sense capacitor plate were covered with PDMS. This causes a rather large spring constant, according to equation (10), resulting in a relatively low sensitivity. Future sensors will be provided with patterned PDMS layers, so the sensitivity will be increased dramatically. This higher sensitivity has already been shown with previous versions of the highly symmetrical accelerometer, realised using a more complicated assembly procedure [7,11]. One of the prototypes with a higher sensitivity was used in a clinical application, namely the measurement of the stability of standing [12].

CONCLUSIONS

A highly symmetrical cube-shaped easy-to-assemble capacitive triaxial accelerometer has been designed, realised and tested. The outer dimensions of the sensor are $5 \times 5 \times 5 \text{ mm}^3$ and the device is put upon a standard IC package. New aspects of the sensor are an easy assembly procedure, the use of the polymers polydimethylsiloxane (PDMS) and polyimide (PI) and the highly symmetrical cubic structure.

The mathematical model, technology and assembly procedure of the sensor were described. The measurement results showed a good linearity in the output voltage for accelerations up to at least 5 g and a bandwidth of DC - >50 Hz. In the x-axis the sensitivity was found to be 175 mV/g which is in good correspondence with the theory. The sensitivity of the y- and z-axis, 55 mV/g and 17 mV/g, respectively, was less than predicted by the theory.

In the sensor described, the PDMS layer was not patterned because the protective chromium layer could not successfully be deposited on top of the patterned PDMS. The sensitivity can be increased by patterning of the PDMS layer, as shown in previous versions of the triaxial accelerometer.

ACKNOWLEDGMENTS

The authors would like to thank Mr. J.G. Bomer, Mr. A.J. Verloop and Mr. Ed A. Droog for their assistance in device preparation and electronic circuitry and the Dutch Technology Foundation (STW) for its support.

REFERENCES

- [1] A.Th.M. Willemsen, F. Bloemhof, H.B.K. Boom, *Automatic stance-swing phase detection from accelerometer data for peroneal nerve stimulation*, IEEE Transactions on biomedical engineering, Vol. 37, 1990, pp. 1201-1208
- [2] P.H. Veltink, E.G. Olde Engberink, B.J. van Hilten, R. Dunnewold, C. Jacobi, *Towards a new method for kinematic quantification of bradykinesia in patients with Parkinson's disease using triaxial accelerometry*, on CD ROM proceedings of IEEE EMBS conference, Montreal, Canada, September 1995
- [3] J.C. Lötters, W. Olthuis, P.H. Veltink, P. Bergveld, *On the design of a triaxial accelerometer*, Journal of Micromechanical Microengineering, 5 (1995), pp. 128-131
- [4] K. Jono, M. Hashimoto, M. Esashi, *Electrostatic servo system for multi-axis accelerometers*, Proceeding IEEE MEMS, 1994, pp. 251-256
- [5] T. Mineta, S. Kobayashi, Y. Watanabe, S. Kanauchi, I. Nakagawa, E. Suganuma, M. Esashi, *Three-axis capacitive accelerometers with uniform axial sensitivities*, Proceedings Transducers'95, Stockholm, Sweden, 1995, pp. 554-557
- [6] J.C. Lötters, W. Olthuis, P.H. Veltink, P. Bergveld, *A sensitive differential capacitance to voltage converter for sensor applications*, submitted to IEEE Instrumentation and Measurement techniques
- [7] J.C. Lötters, W. Olthuis, P.H. Veltink, P. Bergveld, *The rubberelastic polymer polydimethylsiloxane applied as spring material in micromechanical sensors*, Proceedings of MST'96, Potsdam, Germany, September 1996, pp. 73-78
- [8] J.C. Lötters, W. Olthuis, P.H. Veltink, P. Bergveld, *The mechanical properties of the rubberelastic polymer PDMS for sensor applications*, Proceedings of MME, Barcelona, Spain, 21-22 October 1996, pp. 66-69
- [9] H.V. Jansen, M.J. de Boer, R. Legtenberg, M.C. Elwenspoek, *The black silicon method: a universal method for determining the parameter setting of a fluorine-based reactive ion etcher in deep silicon trench etching with profile control*, Journal of Micromechanics and microengineering, 5 (1995), pp. 115-120
- [10] K. Suzuki, I. Shimoyama, H. Miura, *Insect-model based microrobot with elastic hinges*, Journal of microelectromechanical systems, Vol. 3, no. 1, March 1994, pp. 4-9
- [11] J.C. Lötters, W. Olthuis, P.H. Veltink, P. Bergveld, *Design and feasibility of a symmetrical triaxial capacitive accelerometer for medical applications*, Proceedings of Eurosensors X, Leuven, Belgium, 8-11 September 1996, pp. 441-444
- [12] R.E. Mayagoitia, J.C. Lötters, P.H. Veltink, H. Hermens, P. Bergveld, *Standing stability for clinical applications using a triaxial accelerometer*, submitted to Archives of Physical Medicine and Rehabilitation